https://doi.org/10.5194/egusphere-2023-1351
Preprint. Discussion started: 22 June 2023

Existence and influence of mixed states in a model of vegetation patterns

Lilian Vanderveken[1], Marina Martínez Montero[1], and Michel Crucifix[1]
[1]Earth and Life Institute, Louvain-la-neuve, Belgium
Correspondence: Lilian Vanderveken (lilian.vanderveken@uclouvain.be)

Abstract. The Rietkerk vegetation model is a system of partial differential equations, which has been used to understand the formation and dynamics of spatial patterns in vegetation ecosystems, including desertification and biodiversity loss. Here, we provide an in-depth bifurcation analysis of the vegetation patterns produced by Rietkerk's model, based on a linear stability analysis of the homogeneous equilibrium of the system. Specifically, using a continuation method based on the Newton-Raphson algorithm, we obtain all the main heterogeneous solutions for a given size of the domain. We confirm that inhomogeneous vegetated states can exist and be stable, even for a value of rainfall for which no vegetation exists in the non-spatialized system. In addition, we evidence the existence of a new type of solution, which we called "mixed state", in which the equilibria are always unstable and take the form of a mix of two solutions from the main branches. Although these equilibria are unstable, they influence the dynamics of the transitions between distinct stable states, by slowing down the evolution of the system when it passes close to it. Our approach proves to be a helpful way to assess the existence of tipping points in spatially extended systems and disentangle the fate of the system in the Busse balloon. Overall, our findings represent a significant step forward in understanding the behavior of the Rietkerk model and the broader dynamics of vegetation patterns.

1 Introduction

In semi-arid regions, vegetation tends to be spatially organised around patterns (Barbier et al. (2006) Deblauwe et al. (2008), Deblauwe et al. (2011), Deblauwe et al. (2012)). This phenomenon appears in various parts of the world where water is the limiting factor for plants' growth. Vegetation patterns can be modelled and explained with reaction-diffusion equations (Turing, 1952). In general terms, heterogeneous solutions result from the joint effects of a short-range activation mechanism and long-range inhibition. For vegetation on ferruginous soil in semi-arid regions, the short-range activation effect is related to the positive feedback of vegetation on soil water availability, as vegetation limits water loss by runoff by enhancing water infiltration (Meron, 2015).

The rapid diffusion of surface water, however, acts against vegetation growth on bare soil by limiting water availability. The contrast between slow soil water diffusion and fast surface water diffusion produces the spatial, heterogeneous patterns. The mechanisms are described and captured in the Rietkerk model (Rietkerk et al., 2002). This model features three (prognostic) variables: biomass (B) [$g.m^{-2}$], soil water (W) [mm] and surface water (O) [mm], all are functions of time and space. The

https://doi.org/10.5194/egusphere-2023-1351
Preprint. Discussion started: 22 June 2023

evolution of those quantities are governed by three equations:

$$\begin{aligned}
\frac{\partial B}{\partial t} &= c g_{max} \frac{W\,B}{W + k_1} - dB + D_B \Delta B, \\
\frac{\partial W}{\partial t} &= \alpha O \frac{B + k_2 w_0}{B + k_2} - g_{max} \frac{W\,B}{W + k_1} - r_w W + D_W \Delta W, \\
\frac{\partial O}{\partial t} &= R - \alpha O \frac{B + k_2 w_0}{B + k_2} + D_O \Delta O,
\end{aligned} \tag{1}$$

where Δ is the Laplacian operator and R is the rainfall $[mm.day^{-1}]$. The rainfall is the external forcing of the system which we consider to be a spatially-independent function. The first term in the biomass equation represents water uptake by the plant. The first term in the soil water equation is linked to the infiltration rate of water in the soil that is enhanced by the presence of biomass. The factors in front of the Laplacians (ΔB, ΔW and ΔO)are the diffusion constants of the different quantities. The diffusion constant for surface water is considered to be much bigger than those of biomass and soil water. This contrast is essential for pattern creation. In the following, the values of the parameters are as in (Rietkerk et al., 2002).

As explained above, the existence of reaction-diffusion processes enables stable solutions in the form of patterns. Compared to a system without spatial dynamics, such pattern solutions tend to broaden the range of rainfall compatible with the presence of vegetation.

The classical configuration for analysing such a system of equations uses periodic boundary conditions. A pattern is then defined as a spatially periodic solution of the differential equations. Here, we will consider and analyse in depth a region of the parameter space called the Busse balloon (Busse, 1978). This is the region with heterogeneous solutions, that is, the parameter space admitting at least one stable, spatially periodic solution.

The motivating scientific question comes from the following observation. In a system without spatial dynamics — thus without diffusion — a catastrophic transition occurs between sustained vegetation and bare soil when rainfall decreases below a critical point. The transition point corresponds to a fold bifurcation, and can be qualified as a tipping point (Lenton et al., 2008). Rietkerk (Rietkerk et al., 2021) suggested that spatial dynamics and the existence of the Busse ballon smoothens the transition between full-fledged vegetation and bare-soil. In their terms, the Busse Balloon 'evades' the tipping point. This result implies that spatial dynamics effectively lowers the precipitation threshold above which vegetation can be sustained.

Siteur et al. (Siteur et al., 2014) showed that a Busse balloon appears in the Klaussemeier vegetation model (Klausmeier, 1999), where it occupies a region of the parameter space with lower rainfall than necessary to sustain a homogeneous vegetation. However, the nature of this transition through the Busse Balloon may be complex.

The objective of the present study is to fill this gap, in the idealised context of a spatial domain of one dimension, by characterizing the intermediate states that may emerge during the transition from full vegetation to bare soil, and to examine the dynamics that underlie potential transitions between these states.

Specifically, we provide an in-depth analysis of the Busse balloon, demonstrate the co-existence of multiple solutions for a given rainfall intensity, and foresee the circumstances which may trigger transitions between these different solutions. In that sense, we propose an extension of the work by Zelnik et al. (2013) who computes partially the bifurcation diagram

https://doi.org/10.5194/egusphere-2023-1351
Preprint. Discussion started: 22 June 2023

for Rietkerk's model. We also develop the method for finding solution branches and characterise their stability. Finally, we highlight the existence of another type of solution different than the regular patterns. We call them 'Mixed State' because of their shape and show how they can have an influence on the dynamics of the system.

2 Bifurcation diagram and stability

In this section, we present a method to construct the bifurcation diagram for Rietkerk's model and determine the form of the different solution branches as a function of rainfall.

Linear analysis and Turing zone

The classical approach is to consider, first, the static homogeneous solution. To this end, we define the solution $\bar{B} = B(x,t)$ with $\bar{B}$ a constant in time and space—likewise with the other variables—which satisfy the relationships:

$$0 = cg_{max}\frac{\bar{W}\,\bar{B}}{\bar{W}+k_1} - d\bar{B} \tag{2}$$

$$0 = \alpha O\frac{\bar{B}+k_2w_0}{\bar{B}+k_2} - g_{max}\frac{\bar{W}\,\bar{B}}{\bar{W}+k_1} - r_w\bar{W} \tag{3}$$

$$0 = R - \alpha\bar{O}\frac{\bar{B}+k_2w_0}{\bar{B}+k_2}. \tag{4}$$

The analytical solution is:

$$\bar{P} = c\left(\frac{R}{d} - \frac{k_1r_w}{cg_{max}-d}\right), \tag{5}$$

$$\bar{W} = \frac{dk_1}{cg_{max}-d}, \tag{6}$$

$$\bar{O} = \frac{R((cg_{max}-d)(cR+dk_2) - cdk_1r_w)}{\alpha((cg_{max}-d)(cR+dk_2w_0) - cdk_1r_w)}. \tag{7}$$

$$\tag{8}$$

Physical solutions for positive parameters must be positive, and hence satisfy the relations $cg_{max} > d$ and $R > k_1r_w/(cg_{max}-d)$. The homogeneous solutions without vegetation are, by definition, $\bar{B} = 0$, which imply

$$\bar{W}_0 = \frac{R}{r_w} \tag{9}$$

$$\bar{O}_0 = \frac{R}{w_0\alpha}, \tag{10}$$

which are, again, valid for positive parameters. For the parameters chosen here, the homogeneous vegetated solution exists for $R > 1$ and the non-vegetated solution always exists [1]. Fig. 01 shows these solutions as a function of rainfall R.

[1] The universal existence of the non-vegetated solution does not imply its stability for all values of R.

https://doi.org/10.5194/egusphere-2023-1351
Preprint. Discussion started: 22 June 2023

We now consider the stability of these solutions. Again, following standard practice we consider spatially periodic perturbations as follows:

$$B(x,t) = \bar{B} + \epsilon\delta B(x,t), \tag{11}$$
$$W(x,t) = \bar{W} + \epsilon\delta W(x,t), \tag{12}$$
$$O(x,t) = \bar{O} + \epsilon\delta O(x,t), \tag{13}$$

with

$$\delta B(x,t) = \delta B e^{\Omega t + i\kappa x}, \tag{14}$$
$$\delta W(x,t) = \delta W e^{\Omega t + i\kappa x}, \tag{15}$$
$$\delta O(x,t) = \delta O e^{\Omega t + i\kappa x}. \tag{16}$$

We now introduce the perturbation into the original equations, develop a Taylor expansion for small ϵ and get rid of the 0th order term by using the static homogeneous solutions. The linearised equations obtained can be recast as an eigenvalue problem:

$$A = \begin{pmatrix} d - \frac{cg_{max}\bar{W}}{k_1+\bar{W}} + D_B\kappa^2 & \frac{cg_{max}k_1\bar{B}}{(k_1+\bar{W})^2} & 0 \\ \frac{cg_{max}\bar{W}}{k_1+\bar{W}} + \frac{k_2\alpha(w_0-1)\bar{O}}{(k_2+\bar{B})^2} & r_w + \frac{g_{max}k_1\bar{B}}{(k_1+\bar{W})^2} + D_W\kappa^2 & \frac{\alpha(k_2w_0+\bar{B})}{k_2+\bar{B}} \\ -\frac{k_2\alpha(w_0-1)\bar{O}}{(k_2+\bar{B})^2} & 0 & \frac{\alpha(k_2w_0+\bar{B})}{k_2+\bar{B}} + D_O\kappa^2 \end{pmatrix} \begin{pmatrix} \delta B \\ \delta W \\ \delta O \end{pmatrix} = -\Omega \begin{pmatrix} \delta B \\ \delta W \\ \delta O \end{pmatrix} \tag{17}$$

Every pair of values (R,κ) defines a new eigenvalue problem. It corresponds to the linear dynamics obtained by perturbing a homogeneous solution that exists at a particular value of R with wavenumber κ. We are interested in finding out whether there are values values of (R,κ) for which there exists an exponentially growing solution, thus positive Ω. It is then said that the homogeneous solution for a specific value of R is linearly unstable to perturbations of wavenumber κ. For the eigenvalue problem to have a non-trivial solution, the determinant $det(A+\Omega)$ must be 0. This leads to a cubic equation for Ω:

$$a(R,\kappa)\Omega^3 + b(R,\kappa)\Omega^2 + c(R,\kappa)\Omega + d(R,\kappa) = 0, \tag{18}$$

yielding three roots: $\Omega_1(R,\kappa), \quad \Omega_2(R,\kappa), \quad \Omega_3(R,\kappa)$. Two roots are negative for all physical values of R (real positive) and κ (real). One of them, say Ω_1, is positive in a region of the (R,κ) plane. The countour of this area is shown in Fig. 02 by the black line. This defines the *Turing zone*. Hence, for those values of (R,κ) with positive real part of Ω_1 (inside of the contour) the corresponding homogeneous solution is linearly unstable to inhomogeneous perturbations of wavenumber κ.

Zero modes correspond to marginally non-growing inhomogeneous solutions of the linearised equations and correspond to perturbations with $\Omega = 0$. Their existence usually signals the presence of an instability in the full non-linear model, that can send the system towards an inhomogeneous time-invariant solution in the full nonlinear model. Specifically, Fig. 02 suggests the existence of two zero modes for any value of rainfall comprised between critical bounds 1.0 and 1.25. Such zero modes can satisfy the boundary conditions for a (low) wavenumber that depends on R, and therefore require a domain large enough to develop. If the domain is so small that its fundamental mode is in the stable region ($\kappa \gtrsim 0.6$), it is always stable. In this section,

https://doi.org/10.5194/egusphere-2023-1351
Preprint. Discussion started: 22 June 2023

we found zero modes along the homogeneous branch compatible with a specific domain. Those zero mode indicate the start of inhomogeneous branches. In the following section we will rely on those zero modes to compute solutions to the full non-linear model.

2.1 Bifurcation diagram and continuation method

The analysis in the previous section showed that homogeneous vegetation is linearly unstable against spatially periodic inhomogeneous perturbations on the rain range $1 < R < 1.25$. This linear analysis suggested the existence of static periodic inhomogeneous solutions within the nonlinear system within that range. Now, our focus shifts towards explicitly computing these nonlinear solutions. To achieve this, numerical methods are employed to solve the equations involved.

For the time being we assume a periodic domain with a finite size of $L = 100$m. The choice of the size of the domain influences the number of zero modes exhibited by the corresponding homogeneous solution. This choice coupled with periodic boundary conditions effectively discretize the set of zero modes (Fig. 03). Indeed, setting $\kappa = n\frac{2\pi}{L}$, with n the wavenumber, we find to pairs (κ, R) corresponding to zero modes, with the range $\kappa = [0 : 0.6]$, corresponding to perturbing the homogeneous solution $\bar{S}(R)$ with a perturbation $\delta = \cos(\kappa x)$.

For each pair of (κ, R) in the set of zero modes, we identify the corresponding homogeneous solution $(\bar{S})$ and perturb it with the corresponding perturbation $\delta S\cos(\kappa x)$, and periodic boundary conditions are enforced by setting $\kappa = n\frac{2\pi}{L}$, with n the wavenumber. The perturbed homogeneous solution

$$B_0(x,R) = \bar{B} + \delta B cos(\kappa x), \tag{19}$$

$$W_0(x,R) = \bar{W} + \delta W cos(\kappa x), \tag{20}$$

$$O_0(x,R) = \bar{O} + \delta O cos(\kappa x), \tag{21}$$

is then taken as the first guess input in a Newton-Raphson iteration used for finding the corresponding non-linear inhomogeneous solution.

A this point we need to discretization of the spatial domain into, say, N points. We used $N = 100$. Specifically, the discretized first guess reads $u_0(R) = [B_0(R), W_0(R), O_0(R)] \in \Re^{3N}$ and the algorithm

$$u_{i+1}(R) = u_i(R) - \epsilon J^{-1}(u_i(R)) f(u_i(R)), \tag{22}$$

converges towards the solution $u_S(R)$ with $J(u_i(R))$, the Jacobian matrix of the system and $f(u_i(R))$, the right-hand side as in Eq. 1. The Laplacian is discretized with a periodic pseudospectral method. This solution, $u_S(R)$, is then used as the first guess to solve for the solution with rainfall $R + \delta R$,

$$u_0(R + \delta R) = u_S(R) + \delta u, \tag{23}$$

with $\delta u \ll \epsilon$. This iterative procedure leads to the construction of the full branch of solutions.

Each branch obtained by the above technique is denoted by n between 1 and 9, with n the wavenumber associated with the perturbation. All the branches obtained with this approach are shown in Fig. 04. We now see that the range of rainfall

https://doi.org/10.5194/egusphere-2023-1351
Preprint. Discussion started: 22 June 2023

where vegetation is sustained is much wider than expected from the linear analysis. The linear analysis in the previous section predicted the growth of vegetation patterns in the Turing zone, between $1.0\,mm.day^{-1}$ and $1.25\,mm.day^{-1}$. The analysis of the full non linear system actually reveals time-invariant pattern solutions on branches attached to zero modes in the range 0.5 – 1.3 $mm.day^{-1}$. Although the non-linear solution may differ in shape from the linear perturbation, it is found that wavenumber n used to perturb the homogenous solution describes reasonably well the shape of the pattern along the branch obtained from that perturbation. One such solution is displayed for illustration in Fig. 05. For this particular solution, with wavenumber $n = 2$, the biomass accumulates in two places, and soil water peaks there due to enhanced infiltration rate. Surface water accumulates around those areas.

2.2 Stability analysis

Characterizing the stability of equilibria will further help us to understand the dynamics of the system inside the Busse balloon. The Busse balloon is the region in the space parameter (κ, R) where at least one stable pattern solution exists. It gives a partial information about your system for a given value of R and as we will see in the following the unstable states can be of interest for the dynamics of the system.

The stability of solutions is classically estimated based on the Jacobian matrix evaluated at each solution, positive real parts of the eigenvalues signaling instability.

As a first example, the solution for a rainfall equal to $0.9\,mm.d^{-1}$ of the branch $n = 2$, the associated eigenvalues and the first eigenvector are displayed on Fig.05. The majority of eigenvalues have a negative real part. One eigenvalue has a very small, positive real part (3.10^{-10}), which suggests quasi-neutral stability. Further inspection of the associated eigenvector shows that this quasi-neutrally stable mode is the spatial derivative of the equilibrium pattern. Therefore, it corresponds to a translation mode, which is indeed expected with periodic boundary conditions. Hence, we have a stable pattern which may however translate consistently with the periodic character of the boundary conditions. We therefore attribute the small real part to a numerical artifact (it should be zero) and consider equilibria with positive real part of the highest eigenvalue of the order of 10^{-10} as stable.

This stability analysis is repeated for all the solutions shown in Fig. 04. Stable sections of the branches are drawn in solid lines, and unstable ones with dashed lines. This gives us a more precise idea about what is happening inside the Busse balloon. We now know what is the shape of those stable states, and how and at what rainfall value they lose stability. The existence of multiple stable states for a given value of rainfall is also consistent with previous work based on models and real systems (Bel et al. (2012),Bastiaansen et al. (2018))

Some branches of solutions, such was $n = 5, 6, 7, 8, 9$ are unstable in all their existence domain. Other branches, as $n = 1, 2, 3, 4$, change stability along the branch. These branches of solutions, start as unstable from the low vegetation zero modes on the homogeneous solution. Then, they become stable, and eventually become unstable again shortly before joining the highly vegetated homogeneous solution at the corresponding zero mode. The change in stability may take place at the extreme rain values for which the solution exists, as in the $n = 1$ branch, or at a rainfall value in the middle of a branch. As we know, when a solution changes loses stability, the real part of one of its eigenvalues changes from negative to positive, which indicates

https://doi.org/10.5194/egusphere-2023-1351
Preprint. Discussion started: 22 June 2023

that the solution becomes linearly unstable in the direction of the associated eigenvector. In all of the cases here the change of sign of the eigenvalue happens through zero (as opposed to, through infinity), meaning that, there are zero modes at the intersection of the stable and unstable branch sections. As we show next, this may indicate the branching of yet another branch of the full-nonlinear solution.

2.3 "Mixed states"

In the previous section we studied the stability of the "main" branches of solutions shown in Fig. 04. These branches of solutions starting from the zero modes present on the homogeneous vegetated branch. We also saw that some of these branches of solutions had zero modes at the intersection of their stable and unstable parts. These zero modes can act as bifurcation points from which new branches of solutions emerge. The latter can be found by starting from the equilibrium at the bifurcation point, perturbed in the direction of the eigenvector associated with the newly positive eigenvalue (zero mode) corresponding to new an unstable direction. Again, a Newton-Raphson iteration allows us to find the new equilibrium. From there, the continuation method explained in the previous section allows us to trace the full new branch.

The result of this routine applied to the bifurcation point of the branch $n = 4$ is shown on the upper panels of Fig. 06. We see that a new branch begins at the transition between stable and unstable. This branch, which we call $n = 4bis$, is close (regarding to the mean biomass) to that of the $n = 4$ branch and reconnects to the main $n = 4$ branch for higher rainfall. To illustrate the nature of this new branch, solutions for the $n = 4$ and the $n = 4bis$ branches with two values of rainfall are shown on the lower panels of Fig.06,. For a given value of rainfall, the $n = 4bis$ solution looks like a modulation of the $n = 4$ solution by a an other wavenumber. Solutions branching out of zero modes in the homogeneous solution tend to exhibit a single perturbation mode, see Fig. 05. By contrast, solutions branching out of zero modes in those inhomogeneous solutions exhibit a mixture of modes (lower panels of Fig. 06), hence the name "mixed-states". The states along the mixed-state branch $n = 4bis$ are unstable, with positive eigenvalues.

There are numerous mixed-state branches, obtained from the different bifurcation points found along the main branches. These can also be found to emerge from zero modes present on the unstable sections of the main branches. For example, in the low vegetated unstable part of the $n = 2$ branch (see Fig. A2), we find two zero modes at the same value of rainfall, from which two mixed state branches emerge: one labelled $n = 2bis$ because it connects to the $n = 2$ branch and one labelled $n = 3loc$ which connects to the $n = 4$ branch. The $n = 1$ main branch is a special branch in two ways. Firstly, as Zelnik et al. (2013) stated, it is the only stable localized state. Secondly, it starts from a zero mode on the homogeneous solution, but it ends up connecting to the $n = 2$ branch as if it was a "mixed-state", see Fig. A1. The evolution of the shape along this branch goes from 1 localised vegetation peak to 2 localised vegetation peaks in the unstable part close to the connection with the $n = 2$ branch.

All mixed state branches share similar characteristics, with states appearing as a modulation of a main branch. Even though they are unstable, we expect mixed-state modes to influence the dynamics of nearby trajectories, depending on the value of the positive eigenvalue.

https://doi.org/10.5194/egusphere-2023-1351
Preprint. Discussion started: 22 June 2023

3 Numerical simulations of trajectories

To assess relevance of the bifurcation diagram for understanding transient dynamics, we performed two series of numerical simulations.

3.1 Random initial conditions with a fixed rainfall

Here, our objective is to verify that the stable pattern branches act as attractors in the dynamics of the system. To this end we specify a value of rainfall for which which multiple stable solutions exist. Starting with different initial conditions and evolving the system, we expect that different runs end in some of the different available stable states for the chosen rain value. To avoid favoring the attraction to a particular branch we opt for bare soil initial conditions with random noise. Rainfall is set to $R = 1.1\,mm/year$, for which the system has several stable equilibria (n = 2,3 and 4). The model is run for 5000 days with 500 distinct random initial conditions. Those are random from a uniform distribution (positive) noise on top of a homogeneous zero state. Trajectories, projected onto a summary space (mean and maximum biomass) are shown in Fig. 07. As this is a summary space—a projection of the full space—trajectories may appear to cross, but they do not in the full space. Out of the 500 runs, 465 land on the $n = 2$ equilibrium, and the others land on the $n = 3$ equilibrium. This indicates that the equilibria that we identify as stable are the indeed those which attract trajectories. Having no trajectories on the $n = 4$ equilibrium suggests that the basin of attraction of the latter is narrow, with few chances for a trajectory starting from random initial conditions to be in the basin of attraction of that solution or, in more informal terms, to evolve such as to pass close enough to the $s = 4$ solution and land on it. The $n = 4$ equilibrium can however be reached with carefully designed initial conditions, such as a cosine with a wavenumber equal to $n\frac{2\pi}{L}$.

3.2 Effect of a "Mixed State" on the evolution

Here we address the question of whether unstable mixed-state solutions are also able to influence system transient trajectories. In this case the rainfall is set to a $R = 1.05\,mm/year$, for which a mixed-solution exists.

The initial condition is an unstable equilibrium $n = 5$ with a small perturbation along the direction of the first eigenvector. Fig. 08 summarises the evolution of the biomass pattern over time and the corresponding trajectory in summary-space. There we see that the system quite slowly leaves the $n = 5$ unstable equilibria. This is due to the fact that even though the state is unstable, the associated eigenvalues are positive but small. So the dynamics around the equilibrium are slow. After abruptly departing from the $n = 5$ equilibrium, one biomass bump disappears, leading to a rearranged state that approaches a mixed state of $n = 4bis$. That equilibrium is unstable, but the system lingers in its vicinity for a considerable period of time before another bump of biomass vanishes, propelling the system towards the stable equilibrium of $n = 3$. Switching from one state to an other by losing one or more vegetation bumps is a known feature of vegetation patterns model (Bastiaansen and Doelman (2019),Bastiaansen et al. (2020)). The time spent close to the different unstable equilibria is consistent with the leading eigenvalues and the timescales associated of the Jacobian matrix evaluated at the equilibrium. Those eigenvalues and timescales are given in the

https://doi.org/10.5194/egusphere-2023-1351
Preprint. Discussion started: 22 June 2023

	$n = 5$	$n = 4bis$
highest eigenvalues	0.001, 0.001, 0.0002	0.0033 , 0.0033 ,$9\,10^{-9}$
timescales	1000 , 1000, 4980	290, 310, 10^9

Table 1. Eigenvalues and associated timescales for two unstable states

table 1. There is a factor 0.3 between the shortest timescales for $n = 4bis$ and $n = 5$. The experiment shown in Fig. 08 exhibits the same factor between the time spent in the $n = 5$ equilibrium and $n = 4bis$.

4 Discussion

We uncovered the existence of mixed states in Ritkerk's model and shown their importance for transient dynamics. As far as we are aware, such mixed states have never been identified nor described in models for vegetation patterns.

Mixed states emerge at the transition between unstable and stable states along a branch of solutions, and have a functional form that appears as the combination of two solutions from the main branches. We found that while these equilibria are unstable, they may still influence the system's dynamics by slowing down its evolution when it passes near them. The influence of unstable modes on neighbouring dynamics is well-known in complex systems (Lucarini and Bódai, 2017), but it has not been previously reported in the more specific context of transition between vegetation patterns. Further research is needed to determine whether mixed states are a common feature of reaction-diffusion systems.

We adopted periodic boundary conditions, as in previous studies (Rietkerk et al. (2002), Dekker et al. (2007)). As stated by Dijkstra (2011), the periodic boundary conditions allow for the existence of unstable equilibria with high wavenumber. However, this boundary condition, widely used in reaction-diffusion models due to its simplicity and convenience, may not reflect real-world scenarios accurately. More generally, working with a finite-size domain discretises the set of admissible solutions. Hence, the significance of mixed-states for describing the dynamics of infinite-size systems should be assessed.

As a step towards this objective, we computed the bifurcation diagram for a larger domain size of $L = 200$m, instead of $L = 100$m. As expected, we observed more branches in this case but, remarkably, the branches and the stability of the branches shared between the two domains are the same as for $L = 100$ m. The ones with odd n number appear as a consequence of the extended domain. The range of rainfall that can support a stable vegetation pattern also increased slightly with the larger domain size, with the $n = 1$ branch extending this range.

These findings suggest that the existence of mixed-states and their stability properties is reasonably robust accross domain sizes, even though the way they will manifest themselves in continous, large domains is still to be established.

5 Conclusions

We present an in-depth analysis of the Rietkerk model's behavior that we believe sheds a new light on the dynamics of vegetation patterns. Our analysis is based on the bifurcation diagram of the vegetation patterns model, which we constructed

https://doi.org/10.5194/egusphere-2023-1351
Preprint. Discussion started: 22 June 2023

using a variety of techniques. First, we performed a linear stability analysis of the homogeneous equilibrium of the system, which allowed us to delineate the so-called Turing zone. This zone is characterized by the instability of the homogeneous equilibria to small heterogeneous perturbations, and it serves as a starting point for our analysis. Next, we used perturbed states at the edge of the Turing zone, the so-called zero mode, to construct a whole branch of solutions associated with the system. To obtain this branch, we used a continuation method based on the Newton-Raphson algorithm. By doing so, we were able to obtain the heterogeneous solutions for a given size of the domain. As expected, due to the system's non-linearity, we discovered that the system allows for multiple solutions for a given value of parameter, specifically rainfall. We went a step further by assessing the stability of those equilibria by computing the eigenvalues and associated eigenvectors of the Jacobian matrix. This stability analysis showed that inhomogeneous vegetated states can exist and be stable, even for a values of rainfall for which no vegetation exists in the non-spatialized system. Yet, we also found that the main branches of solution originating from a zero mode are not the only ones present in the system. At the transition between unstable and stable states along one branch, a new type of solution appears. In the latter, which we called "mixed state", the equilibria are always unstable and they look like a mix of two solutions from the main branches. Although these equilibria are unstable, they affect on the dynamics by slowing down the evolution of the system when it passes close to it. This slowing effect is well known for complex systems , but to the best of our knowledge, it had not been previously shown for vegetation patterns. Overall, our approach allowed us to construct a bifurcation diagram that gives us valuable insights about the behavior of the system. This approach is helpful to disentangle the fate of the system in the Busse balloon and could be used to assess the existence or not of tipping points in spatially extended systems.

Code availability. All the code used to produce the figures for this manuscript are available here: https://github.com/lvanderveken/Rietkerk_bif_diag

Author contributions. LV, MC and MM designed the study. LV and MM performed the numerical analysis. LV wrote the manuscript and MC and MM reviewed and edited the paper.

Competing interests. The contact author has declared that none of the authors has any competing interests

Acknowledgements. This project has received funding from the European Union's Horizon 2020 research and innovation programme under grant agreement no. 82097. Michel Crucifix is funded as Research Director by the Belgian National Fund of Scientific Research. The authors use chat-GPT3.5 to help rephrasing some parts of the manuscript.

https://doi.org/10.5194/egusphere-2023-1351
Preprint. Discussion started: 22 June 2023

References

Barbier, N., Couteron, P., Lejoly, J., Deblauwe, V., and Lejeune, O.: Self-organized vegetation patterning as a fingerprint of climate and human impact on semi-arid ecosystems, Journal of Ecology, 94, 537–547, https://doi.org/10.1111/j.1365-2745.2006.01126.x, 2006.

Bastiaansen, R. and Doelman, A.: The dynamics of disappearing pulses in a singularly perturbed reaction–diffusion system with parameters that vary in time and space, Physica D: Nonlinear Phenomena, 388, 45–72, https://doi.org/10.1016/j.physd.2018.09.003, 2019.

Bastiaansen, R., Jäibi, O., Deblauwe, V., Eppinga, M. B., Siteur, K., Siero, E., Mermoz, S., Bouvet, A., Doelman, A., and Rietkerk, M.: Multistability of model and real dryland ecosystems through spatial self-organization, Proceedings of the National Academy of Sciences of the United States of America, 115, 11 256–11 261, https://doi.org/10.1073/pnas.1804771115, 2018.

Bastiaansen, R., Doelman, A., Eppinga, M. B., and Rietkerk, M.: The effect of climate change on the resilience of ecosystems with adaptive spatial pattern formation, Ecology Letters, 23, 414–429, https://doi.org/10.1111/ele.13449, 2020.

Bel, G., Hagberg, A., and Meron, E.: Gradual regime shifts in spatially extended ecosystems, Theoretical Ecology, 5, 591–604, https://doi.org/10.1007/s12080-011-0149-6, 2012.

Busse, F. H.: Non-linear properties of thermal convection, Reports on Progress in Physics, 41, 1929–1967, https://doi.org/10.1088/0034-4885/41/12/003, 1978.

Deblauwe, V., Barbier, N., Couteron, P., Lejeune, O., and Bogaert, J.: The global biogeography of semi-arid periodic vegetation patterns, Global Ecology and Biogeography, 17, 715–723, https://doi.org/10.1111/j.1466-8238.2008.00413.x, 2008.

Deblauwe, V., Couteron, P., Lejeune, O., Bogaert, J., and Barbier, N.: Environmental modulation of self-organized periodic vegetation patterns in Sudan, Ecography, 34, 990–1001, https://doi.org/10.1111/j.1600-0587.2010.06694.x, 2011.

Deblauwe, V., Couteron, P., Bogaert, J., and Barbier, N.: Determinants and dynamics of banded vegetation pattern migration in arid climates, Ecological Monographs, 82, 3–21, https://doi.org/10.1890/11-0362.1, 2012.

Dekker, S. C., Rietkerk, M., and Bierkens, M. F.: Coupling microscale vegetation-soil water and macroscale vegetation-precipitation feedbacks in semiarid ecosystems, Global Change Biology, 13, 671–678, https://doi.org/10.1111/j.1365-2486.2007.01327.x, 2007.

Dijkstra, H. A.: Vegetation pattern formation in a semi-arid climate, International Journal of Bifurcation and Chaos, 21, 3497–3509, https://doi.org/10.1142/S0218127411030696, 2011.

Klausmeier, C. A.: Regular and Irregular Patterns in Semiarid Vegetation, Science, 284, 1826–1828, https://doi.org/10.1126/science.284.5421.1826, 1999.

Lenton, T. M., Held, H., Kriegler, E., Hall, J. W., Lucht, W., Rahmstorf, S., and Schellnhuber, H. J.: Tipping elements in the Earth's climate system, Proceedings of the National Academy of Sciences, 105, 1786–1793, https://doi.org/10.1073/pnas.0705414105, 2008.

Lucarini, V. and Bódai, T.: Edge states in the climate system: Exploring global instabilities and critical transitions, Nonlinearity, 30, R32–R66, https://doi.org/10.1088/1361-6544/aa6b11, 2017.

Meron, E.: Nonlinear physics of ecosystems, https://doi.org/10.1201/b18360, 2015.

Rietkerk, M., Boerlijst, M. C., van Langevelde, F., HilleRisLambers, R., van de Koppel, J., Kumar, L., Prins, H. H. T., and de Roos, A. M.: Self-Organization of Vegetation in Arid Ecosystems, The American Naturalist, 160, 524–530, https://doi.org/10.1086/342078, 2002.

Rietkerk, M., Bastiaansen, R., Banerjee, S., van de Koppel, J., Baudena, M., and Doelman, A.: Evasion of tipping in complex systems through spatial pattern formation, https://doi.org/10.1126/science.abj0359, 2021.

Siteur, K., Siero, E., Eppinga, M. B., Rademacher, J. D., Doelman, A., and Rietkerk, M.: Beyond Turing: The response of patterned ecosystems to environmental change, Ecological Complexity, https://doi.org/10.1016/j.ecocom.2014.09.002, 2014.

https://doi.org/10.5194/egusphere-2023-1351
Preprint. Discussion started: 22 June 2023

325 Turing, A. M.: The chemical basis of morphogenesis, Philosophical Transactions of the Royal Society of London. Series B, Biological Sciences, 237, 37–72, https://doi.org/10.1098/rstb.1952.0012, 1952.

Zelnik, Y. R., Kinast, S., Yizhaq, H., Bel, G., and Meron, E.: Regime shifts in models of dryland vegetation, Philosophical Transactions of the Royal Society A: Mathematical, Physical and Engineering Sciences, 371, https://doi.org/10.1098/rsta.2012.0358, 2013.

https://doi.org/10.5194/egusphere-2023-1351
Preprint. Discussion started: 22 June 2023

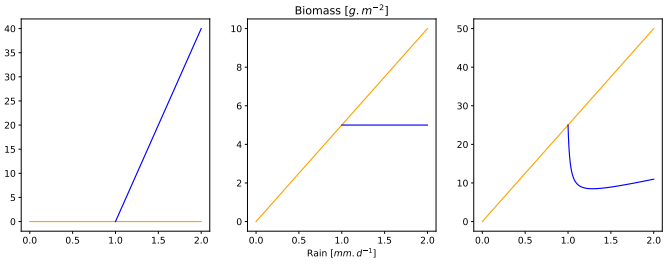

Figure 01. Homogeneous solutions of Rietkerk's model. Blue line is solutions with vegetation, yellow is without.

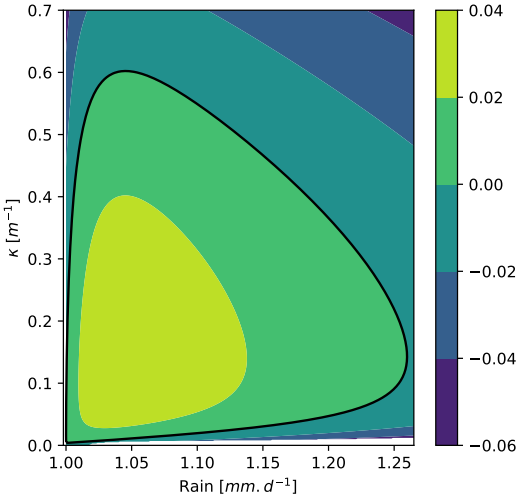

Figure 02. Contour plot for $\Omega_1(R, \kappa)$. The thick black line is the contour $\Omega_1 = 0$ and the region inside that contour corresponds to the parameter region (R, κ) which in which the homogeneous solutions is linearly unstable against inhomogeneous perturbations, i.e., $\Omega > 0$.

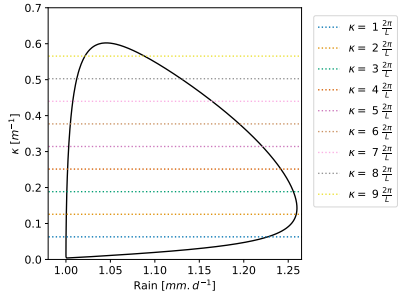

Figure 03. Zero modes present in a domain of $L = 100$. Horizontal lines correspond to harmonics that fit inside the periodic $L = 100$ domain. The intersection of the horizontal lines with the $\Omega_1 = 0$ contour, provides the values of rain R at which new branches of solutions might appear. Notice that each of the 9 horizontal lines that intersect the contour, intersect it twice, hence 18 zero modes.

https://doi.org/10.5194/egusphere-2023-1351
Preprint. Discussion started: 22 June 2023

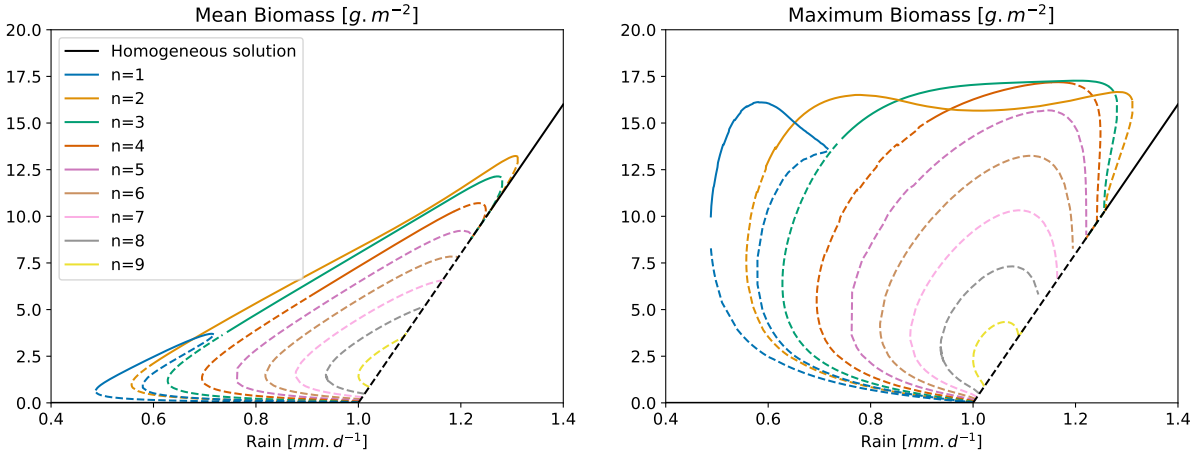

Figure 04. Bifurcation diagram for the Rietkerk's model with $L = 100$m. Each branch is labelled by an integer corresponding to the order of the wavenumber associated with the zero mode. Solid lines correspond to stable states and dashed lines to unstable states.

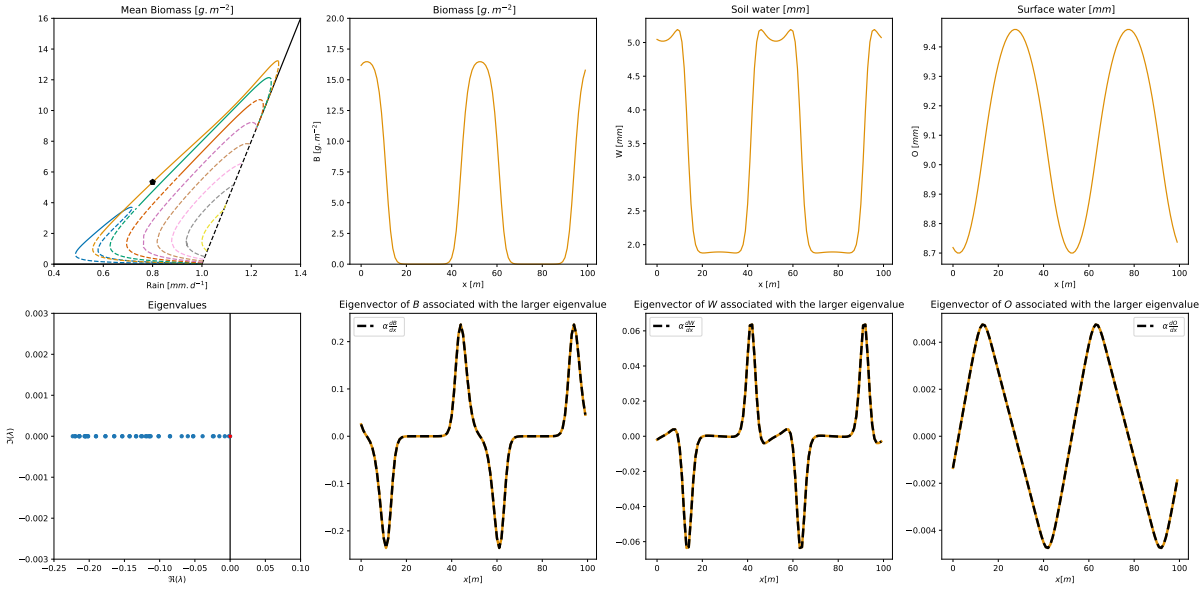

Figure 05. On the upper panels, equilibrium solution for a given value of R (rainfall) ($0.9\,mm.day^{-1}$) on the $n = 2$ branch. The black pentagon on the left-hand-side panel shows the position of the solution on the bifurcation diagram. The three other panels show, from left to right, B (biommass) [$g.m^{-2}$], W (soil water) [mm] and O (surface water) [mm]. On the left-hand-side lower panel,eigenvalues of the Jacobian matrix associated with the solution. The larger eigenvalue is represented wit ha red dot. The three other lower panels show, from left to right, the eigenvector associated with the larger eigenvalue projected on B (biommass), W (soil water) and O (surface water) and with a dashed black line, the first spatial derivative of the solution rescaled.

https://doi.org/10.5194/egusphere-2023-1351
Preprint. Discussion started: 22 June 2023

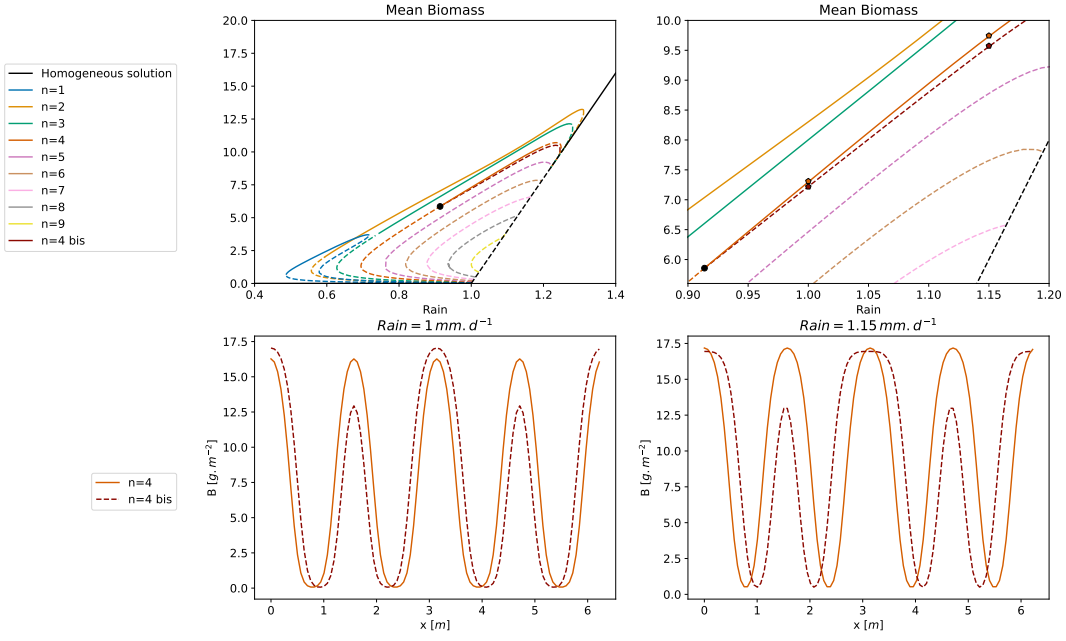

Figure 06. On the left-hand-side upper panel, bifurcation diagram with the addition of a mixed state branch. The bifurcation point is marked with a black dot. On the right-hand-side upper panel, an enhancement of the area around the bifurcation point. On the lower panels, solutions for two values of rainfall of the $n = 4$ and the $n = 4bis$ branch. The position on those solutions on the bifurcation diagram are marked by pentagone on the rigth-hand-side upper panel

https://doi.org/10.5194/egusphere-2023-1351
Preprint. Discussion started: 22 June 2023

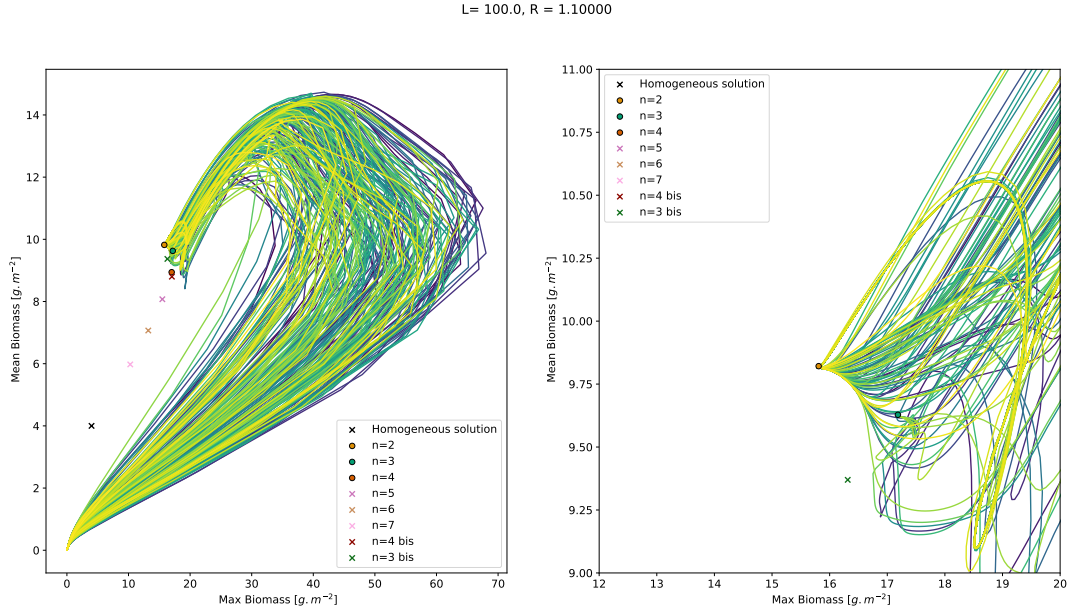

Figure 07. Trajectories on a summary phase space from random initial condition with a fixed rainfall $R = 1,13 mm/year$. The relevant equilibria are shown, if the equilibrium is stable (unstable) the marker associated is a circle (cross).

https://doi.org/10.5194/egusphere-2023-1351
Preprint. Discussion started: 22 June 2023

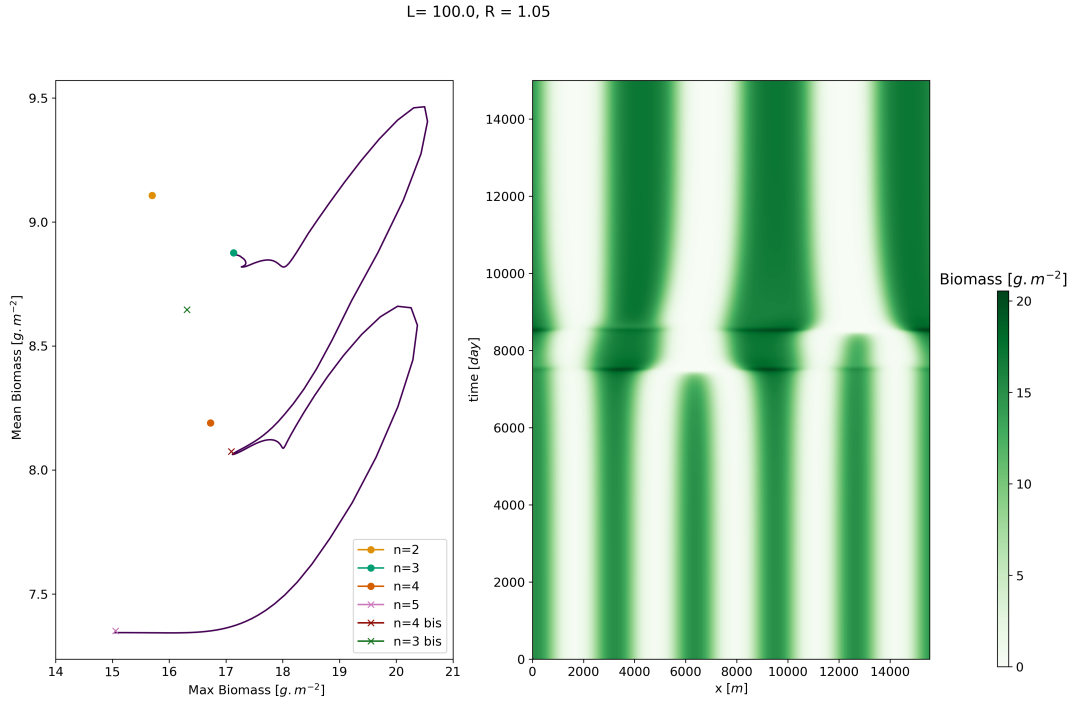

Figure 08. On the left panel, trajectories on a pseudo phase space from an initial condition close to the $n = 5$ equilibrium with a fixed rainfall $R = 1,05mm/year$. On the right panel, we show the time evolution of the biomass

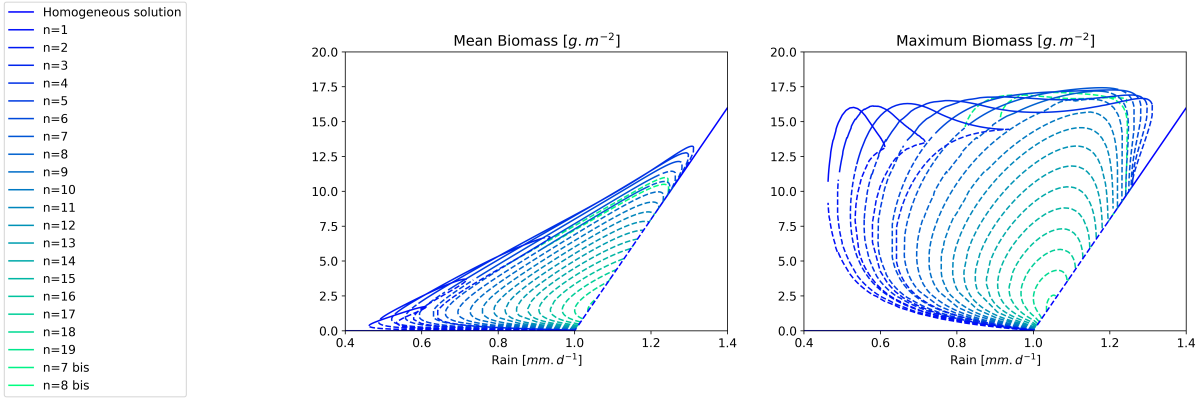

Figure 09. Bifurcation diagram for the Rietkerk's model with $L = 200$m. Each branch is labelled by an integer corresponding to the order of the wavenumber associated with the zero mode. Plain lines correspond to stable states and dashed lines to unstable states.

https://doi.org/10.5194/egusphere-2023-1351
Preprint. Discussion started: 22 June 2023

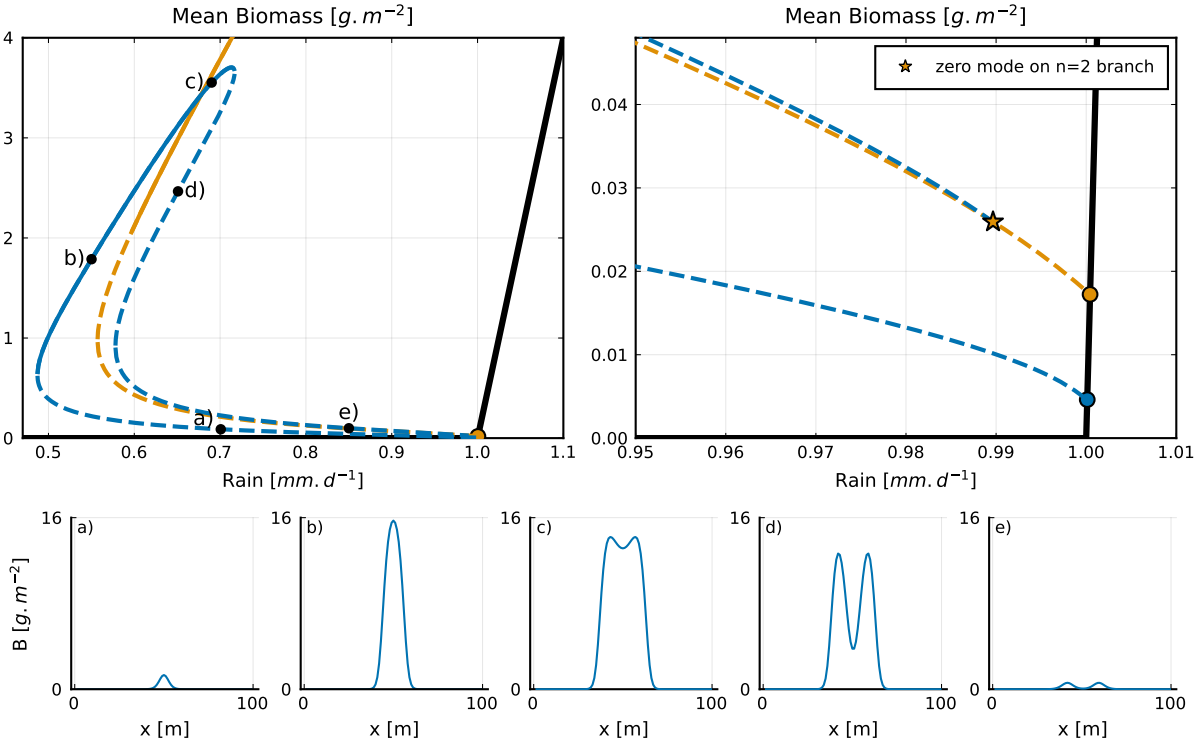

Figure A1. A focus in the bifurcation diagram on the $n = 1$ and $n = 2$ branches; the stable (unstable) states are noted with a (dashed) line. On the left-hand side upper panel, a zoom in the area of the bifurcation diagram where the $n = 1$ branch connects with the $n = 2$ branch. This connection is represented by a star. On the lower panels, solutions along the $n = 1$ branch are shwon. Each corresponds to a black dot in the rigth-hand side upper panel.

https://doi.org/10.5194/egusphere-2023-1351
Preprint. Discussion started: 22 June 2023

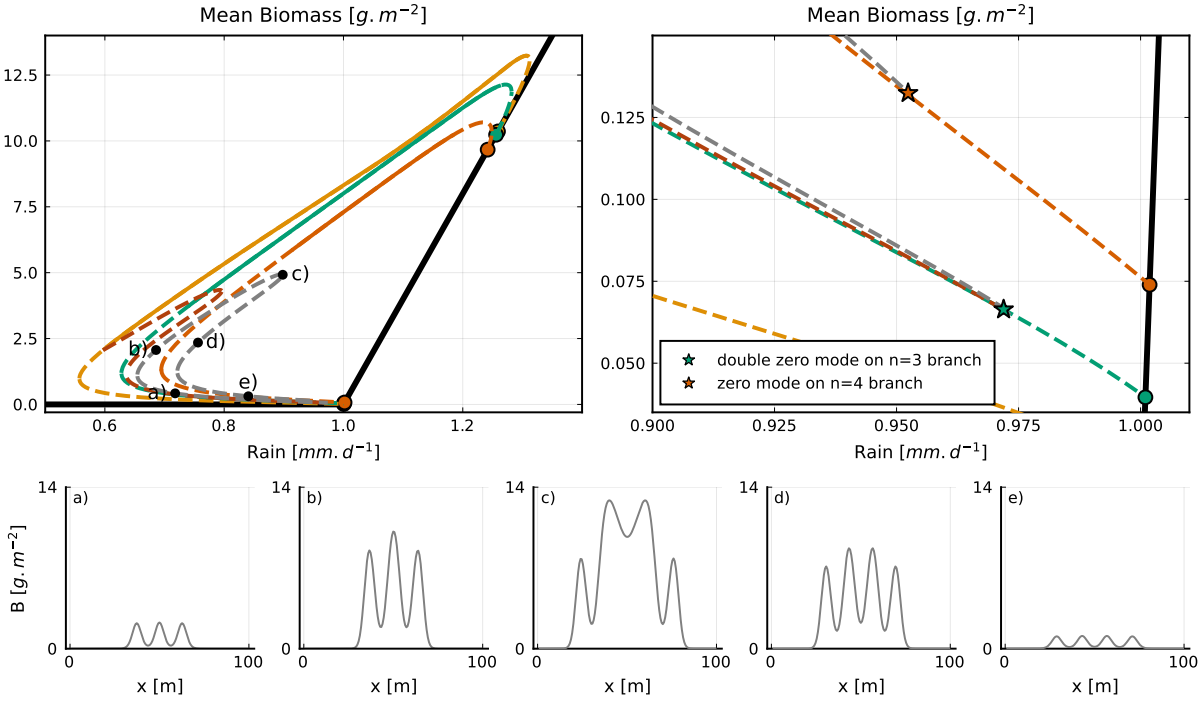

Figure A2. A focus in the bifurcation diagram on the $n = 2$, $n = 2bis$, $n = 3$, $n = 3loc$ and $n = 4$ branches; the stable (unstable) states are noted with a (dashed) line. On the left-hand side upper panel we show a zoom of the bottom part of the bifurcation diagram. The $n = 3$ branch exhibits a double zero-mode, indicated by the green star. Two solutions emerge from that double-zero mode, the $n = 2bis$ and the $n = 3loc$. The first one, connects with the $n = 2$ branch while the second one connects with the $n = 4$ branch at the zero mode indicated by the orange star. On the lower panels, solutions along the $n = 3loc$ branch are shown. Each corresponds to a black dot in the rigth-hand side upper panel.